UNIVERSITY OF SZEGED

Malaria dynamics with long latent period in hosts

by
Kyeongah Nah

Supervisor:
Gergely Röst

A thesis submitted for the
degree of Doctor of Philosophy

in the
Bolyai Institute
Doctoral School in Mathematics and Computer Science

June 2015

INTRODUCTION

The incubation period of malaria can vary depending on the species of parasite or the geographic regions. In particular, in endemic areas of temperate climate (for example in Korea), the incubation period of *Plasmodium vivax* shows bimodal distribution of short and long-term incubation periods. Assuming fixed length for the long-term incubation period (DDE) gives a distribution that is much closer to the empirical distribution, than the exponentially distributed long-term incubation period (ODE).

We compare two transmission models for *P. vivax* malaria, where we model the long-term incubation period using ordinary differential equations or delay differential equations. We identify the basic reproduction number R_0 and show that it is a threshold parameter for the global dynamics of the model. For the DDE model, the global analysis is performed using persistence theory and Lyapunov functionals. We show that, while the qualitative behaviors of the two models are similar, the ODE model overestimates the basic reproduction number and also the level of endemicity, compared to the DDE model. By calculating R_0, we can see that long incubation time is not beneficial to the parasite in a constant environment, thus its presence is connected to the seasonal mosquito activity in Korea. In contrast to the autonomous case, when we incorporate seasonality into our model equations, the interplay of the time delay and the periodicity results that in some situations the DDE model predicts higher prevalence of malaria. The periodic DDE model is also superior to periodic ODE in capturing the qualitative properties of the observed Korean malaria time series, while its mathematical analysis is rather challenging.

Motivated by the addressed problem, we study linear scalar delay differential equations with a single delay and positive periodic coefficients. It is known that if the period is an integer multiple of the delay, then there is a stability threshold expressed by the time average of the coefficients. Under certain conditions, we generalize this principle to situations when the delay and the period do not have to be related. However, it will be shown by examples that in general, this quantity does not determine stability. Such stability result has importance for many systems arisen in mathematical biology.

The prolonged incubation time of *P. vivax* malaria in temperate region is considered to be an adaptation strategy to the seasonal environment. We present evolutionary models of the pathogen in a seasonal

environment. By adaptive dynamics, we explore the direction of the evolution depending on mosquito season length.

P. VIVAX TRANSMISSION WITH LONG INCUBATION PERIOD

To describe the transmission of *P. vivax* malaria, we assume SEIRS disease dynamics for the human and SI for the mosquito population. Exposed humans are divided into two classes by having short-term or long-term incubation periods. If a susceptible human (s_{H}) is successfully infected by a mosquito (i_{M}), then this individual goes through short incubation period (e^s_{H}) with probability p, or long incubation period (e^l_{H}) with probability $1-p$; then becomes infectious (i_{H}) after this incubation time and be able to infect susceptible mosquitoes (s_{M}). Recovered humans are in the class r_{H}, and return to s_{H} after their immunity wanes. We first introduce the ODE system

$$\begin{cases} \frac{ds_H}{dt} = \xi - \alpha s_H i_M + \omega r_H - \xi s_H, \\ \frac{de^s_H}{dt} = p\alpha s_H i_M - d_s e^s_H - \xi e^s_H, \\ \frac{de^l_H}{dt} = (1-p)\alpha s_H i_M - d_l e^l_H - \xi e^l_H, \\ \frac{di_H}{dt} = d_s e^s_H + d_l e^l_H - r i_H - \xi i_H, \\ \frac{dr_H}{dt} = r i_H - \omega r_H - \xi r_H, \\ \frac{ds_M}{dt} = \mu - \beta s_M i_H - \mu s_M, \\ \frac{di_M}{dt} = \beta s_M i_H - \mu i_M, \end{cases} \tag{1}$$

where $\alpha := abm$ and $\beta := ac$. The cross-infection between mosquitoes and humans is described by the terms $abms_{\mathrm{H}}i_{\mathrm{M}}$ and $acs_{\mathrm{M}}i_{\mathrm{H}}$, where a is the per capita biting rate of mosquitoes with transmission efficiency b, c, and m is the proportion of mosquito population to human population. The terms ξ and μ are mortality rates of humans and mosquitoes, respectively; r is the recovery rate and ω is the rate of loss of immunity; $d_s(d_l)$ is the rate of progression from the short (long) term exposed state to the infectious state. With positive parameter values, the feasible domain

$$\{(s_{\mathrm{H}}, e^s_{\mathrm{H}}, e^l_{\mathrm{H}}, i_{\mathrm{H}}, r_{\mathrm{H}}, s_{\mathrm{M}}, i_{\mathrm{M}}) \in \mathbb{R}^7_+ | s_{\mathrm{H}} + e^s_{\mathrm{H}} + e^l_{\mathrm{H}} + i_{\mathrm{H}} + r_{\mathrm{H}} = 1, s_{\mathrm{M}} + i_{\mathrm{M}} = 1\}$$

is invariant.

We define the basic reproduction number R_o for the ODE model by

$$R_o = \sqrt{\frac{\alpha\beta}{(r+\xi)\mu}\left(p\frac{d_s}{d_s+\xi} + (1-p)\frac{d_l}{d_l+\xi}\right)},$$

which has the usual biological interpretation. We show that R_o works as a threshold for the existence and stability of equilibria of system (1). To find equilibria, we set the LHS of system (1) to zero, and solve the algebraic equations.

Lemma 1. *The disease free equilibrium (DFE)* $(1,0,0,0,0,1,0)$ *of system* (1) *always exists. An endemic equilibrium (EE) exists if and only if* $R_o > 1$ *and it is given by the following relations:*

$$i_H = \frac{R_o^2 - 1}{\frac{\beta}{\mu} + K_o R_o^2}, \quad e_H^s = \frac{\frac{p}{d_s+\xi}(r+\xi)}{p\frac{d_s}{d_s+\xi} + (1-p)\frac{d_l}{d_l+\xi}} i_H, \quad e_H^l = \frac{1-p}{d_l+\xi}\frac{d_s+\xi}{p} e_H^s,$$

$$r_H = \frac{r}{\omega+\xi} i_H, \quad i_M = \frac{\frac{\beta}{\mu} i_H}{1+\frac{\beta}{\mu} i_H}, \quad s_H = 1 - e_H^s - e_H^l - i_H - r_H,$$

and $s_M = 1 - i_M$, *where* $K_o = \frac{\frac{p}{d_s+\xi} + \frac{1-p}{d_l+\xi}}{p\frac{d_s}{d_s+\xi} + (1-p)\frac{d_l}{d_l+\xi}}(r+\xi) + 1 + \frac{r}{\omega+\xi}$.

The local asymptotic stability of the DFE can be demonstrated by standard linearization: one can compute the characteristic equation, and show that if $R_o < 1$, all roots of the characteristic equation have negative real parts and if $R_o > 1$, there exist a positive real root.

Theorem 1. *The DFE of system* (1) *is locally asymptotically stable if* $R_o < 1$ *and is unstable if* $R_o > 1$.

Now we introduce a DDE model assuming the long incubation period has a fixed length, τ:

$$\begin{cases} \frac{ds_H}{dt} = \xi - \alpha s_H i_M + \omega r_H - \xi s_H, \\ \frac{de_H^s}{dt} = p\alpha s_H i_M - d_s e_H^s - \xi e_H^s, \\ \frac{di_H}{dt} = d_s e_H^s + (1-p)\alpha s_H(t-\tau) i_M(t-\tau) e^{-\xi\tau} - r i_H - \xi i_H, \\ \frac{dr_H}{dt} = r i_H - \omega r_H - \xi r_H, \\ \frac{ds_M}{dt} = \mu - \beta s_M i_H - \mu s_M, \\ \frac{di_M}{dt} = \beta s_M i_H - \mu i_M. \end{cases} \tag{2}$$

Note that $e_{\mathrm{H}}^{l}(t)$ does not appear in the right hand side of the system (2) and the state space can be specified as

$$\Omega := C\left([-\tau,0],\mathbb{R}\right)\times\mathbb{R}^4\times C\left([-\tau,0],\mathbb{R}\right),$$

where $C\left([-\tau,0],\mathbb{R}\right)$ is the space of real valued continuous functions on the interval $[-\tau,0]$. For solutions in Ω, we introduce a notation, $x_t := (s_{\mathrm{H}t}, e_{\mathrm{H}}^{s}(t), i_{\mathrm{H}}(t), r_{\mathrm{H}}(t), s_{\mathrm{M}}(t), i_{\mathrm{M}t}) \in \Omega$, where $s_{\mathrm{H}t} \in C\left([-\tau,0],\mathbb{R}\right)$ and $i_{\mathrm{M}t} \in C\left([-\tau,0],\mathbb{R}\right)$ are defined by the relations $s_{\mathrm{H}t}(\theta) = s_{\mathrm{H}}(t+\theta)$, $i_{\mathrm{M}t}(\theta) = i_{\mathrm{M}}(t+\theta)$ for $\theta \in [-\tau,0]$. We write $\hat{y}$ for the element of $C\left([-\tau,0],\mathbb{R}\right)$ satisfying $\hat{y}(\theta) = y$ for all $\theta \in [-\tau,0]$. Let

$$\Omega_+ := C\left([-\tau,0],\mathbb{R}_+\right)\times\mathbb{R}_+^4\times C\left([-\tau,0],\mathbb{R}_+\right).$$

Following the biological interpretation of our system, we prescribe initial condition as

$$x_0 = \phi_0 \in \Omega_+. \tag{3}$$

Then system (2) can be written in the abstract form

$$\frac{dx(t)}{dt} = \mathcal{F}(x_t),$$

where $\mathcal{F}:\Omega\to\mathbb{R}^6$, with initial condition (3). We consider $\mathbb{R}^6$ equipped with the L^∞ norm and $C\left([-\tau,0],\mathbb{R}\right)$ equipped with the usual supremum norm denoted by $||\cdot||$. Now Ω is a Banach space with the norm

$$|\phi|_\Omega := \max\left\{\|f\|, |q_2|, |q_3|, |q_4|, |q_5|, \|g\|\right\},$$

for

$$\phi = (f, q_2, q_3, q_4, q_5, g) \in \Omega.$$

It is easy to show that $\mathcal{F}$ satisfies the local Lipschitz condition on each bounded subset of Ω, from which the local existence of solutions of (2) follows. Furthermore, it is straightforward to show that $x_t \in \Omega_+$ for sufficiently small t and it is easy to give an a priori bound for $|x_t|_\Omega$. Thus the solution x_t is continuable on $\mathbb{R}_+$. Consequently, (2) with (3) induces a continuous semiflow

$$\Phi : \mathbb{R}_+\times\Omega_+\to\Omega_+,$$

defined by

$$\Phi\left(t,\phi_0\right) = x_t\left(\phi_0\right).$$

Let $X\subset\Omega_+$ to be

$$X := \left\{ \phi \;\middle|\; \begin{array}{l} 0\le f(\theta),\ 0\le g(\theta),\ \text{for } \theta\in[-\tau,0], \\ 0\le q_j,\ j\in\{2,3,4,5\}, \\ f(0) + \int_{-\tau}^{0}(1-p)\alpha f(s)g(s)e^{\xi s}\mathrm{d}s + \sum_{j=2}^{4} q_j = 1, \\ q_5 + g(0) = 1. \end{array} \right\}.$$

Proposition 1. *The set X is forward invariant under Φ, i.e.*

$$\Phi(t, X) \subset X, \ t \in \mathbb{R}_+.$$

In X, the fractions of the human population sum up to 1, with all human compartments $(s_H, e_H^s, e_H^l, i_H, r_H)$ being nonnegative; and the fraction of mosquito populations sum up to 1, with all mosquito compartments (s_M, i_M) being nonnegative. Therefore X is exactly the biologically meaningful state space.

The basic reproduction number R_d of the DDE model is given by

$$R_d = \sqrt{\frac{\alpha\beta}{\mu(r+\xi)}\left((1-p)e^{-\xi\tau} + p\frac{d_s}{d_s+\xi}\right)}.$$

We show that R_d is a stability threshold of system (2).

Lemma 2. *The disease free equilibrium (DFE) $(\hat{1}, 0, 0, 0, 1, \hat{0})$ of system (2) always exists. An endemic equilibrium (EE) exists if and only if $R_d > 1$ and it is given by the following relations:*

$$s_H = \frac{\frac{\beta}{\mu} + K_d}{\frac{\beta}{\mu} + K_d R_d^2}, \quad e_H^s = \frac{p\xi}{(1-p)(d_s+\xi)e^{-\xi\tau} + pd_s}\frac{r+\xi}{\xi} i_H,$$

$$i_H = \frac{R_d^2 - 1}{\frac{\beta}{\mu} + K_d R_d^2}, \quad r_H = \frac{r}{\omega+\xi} i_H, \quad i_M = \frac{\frac{\beta}{\mu} i_H}{1 + \frac{\beta}{\mu} i_H}, \quad s_M = 1 - i_M,$$

$$\text{where} \quad K_d = \frac{\frac{p}{d_s+\xi} + (1-p)\frac{1-e^{-\xi\tau}}{\xi}}{p\frac{d_s}{d_s+\xi} + (1-p)e^{-\xi\tau}}(r+\xi) + 1 + \frac{r}{\omega+\xi}.$$

Theorem 2. *The DFE of system (2) is locally asymptotically stable if $R_d < 1$ and unstable if $R_d > 1$. The EE is locally asymptotically stable whenever exists, i.e. if $R_d > 1$.*

We study the global dynamics of the DDE model.

Theorem 3. *If $R_d \leq 1$, then the DFE is globally attractive in X. Furthermore, if $R_d < 1$ holds, then the DFE is globally asymptotically stable in X.*

The proof includes the construction of a Lyapunov functional and application of LaSalle's invariance principle. Next we study the persistence of the disease for $R_d > 1$. Let us define

$$\rho := \sum_{i=1}^{4} \rho_i,$$

where $\rho_i : X \to \mathbb{R}_+$ for $i \in \{1,2,3,4\}$ are given by

$$\rho_1(\phi) = q_2, \qquad \rho_2(\phi) = (1-p)\alpha \int_{-\tau}^{0} f(s)g(s)e^{\xi s}\mathrm{d}s,$$
$$\rho_3(\phi) = q_3, \qquad \rho_4(\phi) = g(0).$$

Let

$$\tilde{X} := \{\phi \in X | \rho(\phi) > 0\},$$
$$X_0 := \{\phi \in X | \rho(\phi) = 0\} = X \setminus \tilde{X},$$

where X_0 is called the extinction space corresponding to ρ, for obvious reasons: X_0 is the collection of states where the disease is not present.

Proposition 2. *The following assertions hold.*

1. *The set $\tilde{X}$ is forward invariant under Φ. Moreover, for each $i \in \{1,2,3,4\}$ it holds that*
$$\rho_i(\Phi(t,\phi)) > 0 \text{ for } \phi \in \tilde{X} \text{ and } t > \tau.$$

2. *The extinction space X_0 is forward invariant under Φ.*

The proof is based on the comparison method and the method of steps. We now introduce some terminology of persistence theory from [1].

Definition 1. *Let X be a nonempty set and $\rho : X \to \mathbb{R}_+$.*

1. *A semiflow $\Phi : \mathbb{R}_+ \times X \to X$ is called uniformly weakly ρ-persistent, if there exists some $\epsilon > 0$ such that*
$$\limsup_{t\to\infty} \rho(\Phi(t,x)) > \epsilon \quad \forall x \in X,\ \rho(x) > 0.$$

2. *A semiflow Φ is called uniformly (strongly) ρ-persistent, if there exists some $\epsilon > 0$ such that*
$$\liminf_{t\to\infty} \rho(\Phi(t,x)) > \epsilon \quad \forall x \in X,\ \rho(x) > 0.$$

3. *A set $M \subset X$ is called weakly ρ-repelling if there is no $x \in X$ such that $\rho(x) > 0$ and $\Phi(t,x) \to M$ as $t \to \infty$.*

For a function $f : \mathbb{R} \to \mathbb{R}$, we use the notation

$$f_\infty = \liminf_{t\to\infty} f(t).$$

By Proposition 2 and a contradiction argument, we can easily show that the DFE is weakly ρ-repelling when $R_d > 1$. Together with the obvious statement $\cup_{\phi \in X_0} \omega(\phi) = (\hat{1}, 0, 0, 0, 1, \hat{0})$, one can see that Φ is uniformly weakly ρ-persistent using Theorem 8.17 in [1]. Since Φ has a compact global attractor on X, we can apply Theorem 4.5 in [1] to conclude the following:

Theorem 4. *If $R_d > 1$, then the semiflow Φ is uniformly ρ-persistent.*

Using Theorem 4 and the Fluctuation method, we can show that Φ is weakly ρ_4 -persistent. Uniform persistence follows from Theorem 4.5 in [1]. By similar steps, one can also prove Theorem 6.

Theorem 5. *If $R_d > 1$, then Φ is uniformly ρ_4 -persistent.*

Theorem 6. *If $R_d > 1$, then Φ is uniformly ρ_3 -persistent.*

From the first equation of (2), one can see that:

Lemma 3. *There exists $T > 0$ such that $s_{_H}(t) > \frac{1}{2}\frac{\xi}{\alpha+\xi}$ for all $t \geq T$.*

By Proposition 2, together with Theorem 5 and Lemma 3, we obtain lower estimation for $e^s_{_{H\infty}}$. Theorem 8 can be shown in a similar way.

Theorem 7. *If $R_d > 1$, then Φ is uniformly ρ_1 -persistent.*

Theorem 8. *If $R_d > 1$, then Φ is uniformly ρ_2 -persistent.*

Combining Theorems 5, 6, 7, 8 and Proposition 2.1, we obtain:

Corollary 1. *If $R_d > 1$, there exists $\epsilon > 0$ such that*

$$e^s_{_{H\infty}} > \epsilon,\ e^l_{_{H\infty}} > \epsilon,\ i_{_{H\infty}} > \epsilon \ \text{ and } \ i_{_{M\infty}} > \epsilon$$

for every $\phi_0 \in \tilde{X}$, i.e. the disease uniformly persists in each infected compartments of the human and the mosquito populations.

In the special case of $\omega = 0$, which means that individuals acquire permanent immunity after recovering from the infection, we have a result on the global stability of the EE. The proof is rather elaborative, and includes the construction of a Lyapunov functional and the application of LaSalle's invariance principle.

Theorem 9. *Assume that $\omega = 0$. If $R_d > 1$, then the EE is globally asymptotically stable in $\tilde{X}$.*

So far, we have shown that for both ODE and DDE models there exists a threshold value determining the existence and stability of equilibria. Now we compare these threshold values and also the endemic equilibria of the two models.

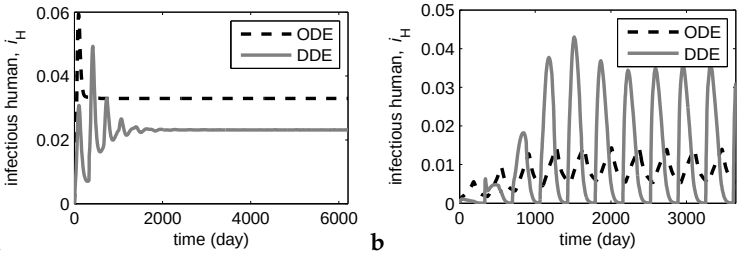

Figure 1: **Dynamics of the infectious human population proportion. a,** Non-seasonal case with constant biting rate. When $R_o > 1$ and $R_d > 1$, $i_H(t)$ converge to endemic equilibrium with $i_o > i_d$. Parameter values are: $\mu = 0.2$, $b = 0.5$, $c = 0.5$, $a = 0.3$, $d_s = 0.04$, $d_l = 0.003$, $r = 0.07$, $p = 0.25$, $\omega = 1/365$, $\xi = 0.004$ and $m = 10$. **b,** Seasonal case with periodic biting rate. In both models, $i_H(t)$ converges to a periodic attractor. The DDE model has a higher peak of infection, moreover, its annual average is also greater than that of the ODE model. Parameter values are $m = 2$, $P = 365$, $L = 365/2$, $a_s = 0.3$, $\xi = 0.00004$, and the other values are the same as in Figure 1a.

Proposition 3. *When all parameters are fixed, the basic reproduction number R_o of the ODE model is greater than the basic reproduction number R_d of the DDE model. Moreover, when $R_d > 1$, i_H^* of the ODE model (denoted by i_o) is greater than i_H^* of the DDE model (denoted by i_d).*

In temperate regions, the transmission of *P. vivax* malaria shows seasonal variation and we incorporate temporal variation into the biting rate, replacing the constant a by

$$a(t) = \begin{cases} a_s & kP \le t < kP + L, \\ 0 & kP + L \le t < (k+1)P, \end{cases}$$

where k is an integer, L is the length for a mosquito season and P is the natural period (one year).

In contrast to the autonomous case, when we incorporate seasonality into our model equations, the interplay of the time delay and the periodicity results that in some situations the DDE model predicts higher prevalence of malaria, see Figure 1. The periodic DDE model is also superior to periodic ODE in capturing the qualitative properties of the observed Korean malaria time series, while its mathematical analysis is rather challenging.

STUDY OF $\dot{x}(t) = -a(t)x(t) + b(t)x(t-1)$

We investigate the scalar periodic delay-differential equation

$$\dot{x}(t) = -a(t)x(t) + b(t)x(t-1), \tag{4}$$

where a, b are assumed to be P-periodic continuous real functions with $a(t) \geq 0$ and $b(t) \geq 0$.

Let $\Omega := C([-1,0], \mathbb{R})$ be the Banach space of real valued continuous functions on $[-1,0]$ with the usual supremum norm. For any $\phi \in \Omega$, a unique solution $x(t;\phi)$ exists for all $t \geq 0$ with

$$x(\theta) = \phi(\theta), \quad -1 \leq \theta \leq 0.$$

From the non-negativity of the coefficients, it follows that the non-negative cone $\Omega_+ := C([-1,0], \mathbb{R}_+)$ is positively invariant, and non-negative solutions remain non-negative. We use the notation $x_t = x_t^\phi \in \Omega$ for the function $x_t(\theta) = x(t+\theta)$, $\theta \in [-1,0]$. Let $\mathcal{U} : \mathbb{R}_+ \times \mathbb{R} \times \Omega \to \Omega$ be the solution operator of (4). That is,

$$\mathcal{U}(t, \sigma, \phi) = x_{t+\sigma},$$

where $x_{t+\sigma}$ is the solution of the initial value problem

$$\begin{aligned} \dot{x}(t) &= -a(t)x_t(0) + b(t)x_t(-1), \quad t \geq \sigma \\ x_\sigma &= \phi \end{aligned}$$

at time $t + \sigma$. We now define the Poincare operator $\mathcal{M} : \Omega \to \Omega$ as

$$\mathcal{M}(\psi) = \mathcal{U}(P, 0, \psi).$$

The stability of zero is determined by the spectral radius of $\mathcal{M}$. Here we derive the explicit threshold formula, determining the stability of zero for (4) using a direct approach. Using a Lyapunov functional and comparison method, we obtain the following results.

Theorem 10. *Let*

$$r := \int_0^P (b(s) - a(s))\, \mathrm{d}s.$$

For Equation (4), the following holds if the sign of $b(u+1) - a(u)$ does not change:

(i) if $r > 0$, zero is unstable;

(ii) if $r = 0$, zero is stable, but not asymptotically stable;

(iii) if $r < 0$, zero is asymptotically stable.

We present a particular example showing that the assumption in Theorem 10 is critical. Consider a special case with constant function $a(t) = \alpha$ and a continuous function $b(t)$ such that

$$\begin{cases} b(t) = 0 \ \text{ if } \ kP \le t \le kP + L, k = 0, 1, 2, \cdots \\ b(t) > 0 \ \text{ elsewhere,} \end{cases} \tag{5}$$

where $1 \le L < P < L + 1$.

Lemma 4. *Consider $b(t)$ in (5). Let*

$$\mathcal{A} := \left\{ \psi \in \Omega \middle| \psi(\theta) = \begin{cases} \psi(-1)e^{-\alpha(1+\theta)} & \text{for} \quad \theta \in [-1, L-P], \\ \psi(-1)e^{-\alpha(1+\theta)} \left(e^{\alpha} \int_{L-P}^{\theta} b(s)\mathrm{d}s + 1 \right) & \\ \qquad\qquad\qquad\qquad \text{for} \quad \theta \in (L-P, 0]. \end{cases} \right\}.$$

Then, $\mathcal{M}(\Omega) \subset \mathcal{A}$. Consequently, $\mathcal{A}$ is forward invariant under $\mathcal{M}$.

Theorem 11. *The zero solution of (4) is stable if and only if $\gamma \le 0$, where*

$$\gamma := -\alpha + \frac{1}{P} \ln \left(e^{\alpha} \int_{L-P}^{0} b(s)\mathrm{d}s + 1 \right),$$

with $b(t)$ defined in (5).

We now address an example where the sign of r does not always coincide with the sign of γ. Consider the special case of (5),

$$b(t) = \begin{cases} 0 \ \text{ if } \ kP \le t \le kP + L \\ \frac{4\beta}{P-L} \left(- \left| t - \frac{P+L}{2} \right| + \frac{P-L}{2} \right) \ \text{ if } \ kP + L \le t \le (k+1)P, \end{cases} \tag{6}$$

where $k = 0, 1, 2, \cdots$. In this case,

$$\gamma = -\alpha + \frac{1}{P} \ln \left(e^{\alpha} \beta (P - L) + 1 \right)$$

and

$$r = \beta(P - L) - \alpha P.$$

There would be four possible cases: (i) $r > 0, \gamma > 0$ (Unstable) (ii) $r < 0, \gamma > 0$ (Unstable), (iii) $r > 0, \gamma < 0$ (Unstable) and (iv) $r < 0, \gamma < 0$ (Stable). Figure 2 shows the parameter sets of each cases. The area with $\gamma < 0$ but $r > 0$, and the area with $\gamma > 0$ but $r < 0$ are the regions where r in (10) does not work as a stability threshold.

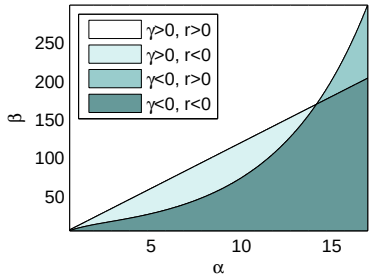

Figure 2: **Special case of (5) with function $b(t)$ as in (6) with $P = 1.2$ and $L = 1.1$.** Distinctive $\alpha - \beta$ parameter regions are determined by the signs of γ and r.

LATENT PERIOD AS AN ADAPTATION STRATEGY TO SEASONAL FORCING

We consider a host-pathogen system in which the pathogens are capable of changing a trait, namely the length of the latent period in the infected host, as a response to seasonal variability. In order to investigate the role of latency in a seasonal environment, we first consider the classic SLIS disease transmission model with periodic seasonal transmission parameter:

$$\begin{cases} \dfrac{dS(t)}{dt} = b(1 - S(t)) - \beta(t)S(t)I(t) + rI(t), \\ \dfrac{dL_1(t)}{dt} = \beta(t)S(t)I(t) - n\theta^{-1}L_1(t) - bL_1(t), \\ \dfrac{dL_j(t)}{dt} = n\theta^{-1}L_{j-1}(t) - n\theta^{-1}L_j(t) - bL_j(t), \quad j = 2, \ldots, n, \\ \dfrac{dI(t)}{dt} = n\theta^{-1}L_m(t) - (r + b)I(t), \end{cases} \tag{7}$$

where S, L and I denote the susceptible, latent and infectious compartments, respectively. To express various distributions of latency in a flexible way, we incorporate multiple latent sub-compartments $L_1, \ldots, L_n$. Such a linear chain represents an Erlang distribution with average θ. Parameters r and b represent the recovery rate and the mortality rate, respectively. We assume that the seasonal driver affects the transmission rate of the pathogen $\beta(t)$ with period P, usually one year. Each year is divided into an on-season, during which the pathogen can be transmit-

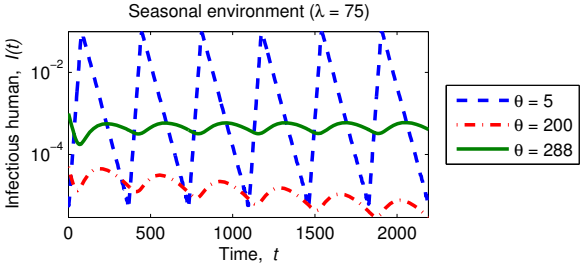

Figure 3: **Infectious host dynamics (7) in seasonal environment with different average length of latent periods**, which shows sharp peak for short latency, extinction for intermediate latency, and moderate oscillation for long latency. Parameter values used in all simulations are $P = 365$, $b = 1/1000$, $r = 1/30$, $n = 3$ and $\beta_* = 0.3$.

ted, and an off-season, during which no new infections can occur. We consider a piecewise constant transmission function,

$$\beta(t) = \begin{cases} \beta_* & kP \le t < kP + \lambda \\ 0 & kP + \lambda \le t < (k+1)P, \end{cases} \tag{8}$$

where λ is the length of on-season, with P being the sum of the lengths of the on-season and the off-season. The time $t = kP$, where k is an integer, corresponds to the beginning of each season.

Figure 3 shows numerical solutions corresponding to three different average lengths of latent periods. In this example, the disease sustains either with short or long latency, but not with intermediate one.

Figure 4 presents numerically calculated R_0, by applying a recently developed approach [2]. We observe two possible profiles depending on seasonal forcing and model parameters: (i) R_0 monotonically decreases with latency; (ii) R_0 has a bimodal shape. Profile (i) is observed in a non-seasonal environment, when the length of on-season is approximately equal to the period. In other cases, we observe profile (ii), the non-monotonicity of R_0 with respect to the length of latent period. In some cases, it leads to die-off intervals of latency: the disease can sustain with short or long latent periods, but not with the medium range of latent periods as in the example of Figure 3. We also observe that solutions with different θ can look dissimilar even though their R_0s are the same.

We characterize infected host individuals by the length of latency, which is the adaptive trait of the parasite that caused the infection. This

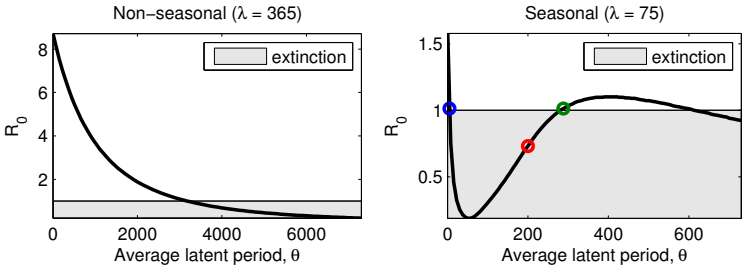

Figure 4: **Qualitatively distinct (θ,R_0)-graphs with various on-season length, λ.** (i) When $\lambda = 365$, R_0 monotonically decreases in θ. (ii) R_0 has a bimodal shape when $\lambda = 75$, and there exists a die-off interval of latent period. R_0 corresponding to $\theta = 200$ (red) is 0.732, and infectious human solution in Figure 3 goes extinct. R_0s corresponding to $\theta = 5$ (blue) and $\theta = 288$ (green) have the same value 1.013, so that the infectious human population persists.

way, the evolution of latency can be studied via a resident-mutant model, describing the competition between the resident and mutant populations:

$$
\begin{aligned}
\frac{dS(t)}{dt} &= b(1-S(t)) - \beta(t)S(t)\left(I_{\mathrm{r}}(t) + I_{\mathrm{m}}(t)\right) + r(I_{\mathrm{r}}(t) + I_{\mathrm{m}}(t)),\\
\frac{dL_{\mathrm{r},1}(t)}{dt} &= \beta(t)S(t)I_{\mathrm{r},1}(t) - n\theta_{\mathrm{r}}^{-1}L_{\mathrm{r},1}(t) - bL_{\mathrm{r},1}(t),\\
\frac{dL_{\mathrm{r},j}(t)}{dt} &= n\theta_{\mathrm{r}}^{-1}L_{\mathrm{r},j}(t) - n\theta_{\mathrm{r}}^{-1}L_{\mathrm{r},j}(t) - bL_{\mathrm{r},j}(t), \quad j = 2,\dots n\\
\frac{dI_{\mathrm{r}}(t)}{dt} &= n\theta_{\mathrm{r}}^{-1}L_{\mathrm{r},n}(t) - (r+b)I_{\mathrm{r}}(t),\\
\frac{dL_{\mathrm{m},1}(t)}{dt} &= \beta(t)S(t)I_{\mathrm{i},1}(t) - n\theta_{\mathrm{m}}^{-1}L_{\mathrm{m},1}(t) - bL_{\mathrm{i},1}(t),\\
\frac{dL_{\mathrm{m},j}(t)}{dt} &= n\theta_{\mathrm{m}}^{-1}L_{\mathrm{m},j-1}(t) - n\theta_{\mathrm{m}}^{-1}L_{\mathrm{m},j}(t) - bL_{\mathrm{m},j}(t), \quad j = 2,\dots n\\
\frac{dI_{\mathrm{m}}(t)}{dt} &= n\theta_{\mathrm{m}}^{-1}L_{\mathrm{m},n}(t) - (r+b)I_{\mathrm{m}}(t),
\end{aligned}
\tag{9}
$$

with lower index **r** standing for resident strain, **m** for invader mutant strain. We investigate which mutant population has the potential to spread and later replace the resident population. When the mutation

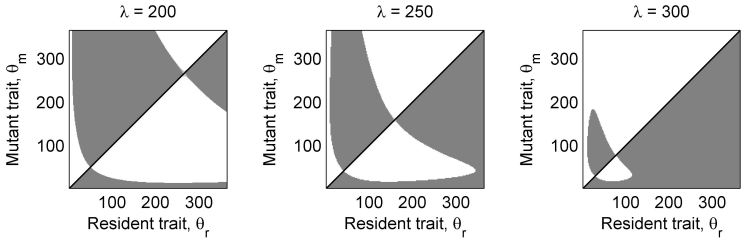

Figure 5: **The long on-season leads to the short latency.** PIPs with on-season length $\lambda = 200$, $\lambda = 250$ and $\lambda = 300$. The longer the on-season, the shorter the gap between two CSSs.

is a rare event, we may assume that the resident population is already settled at an equilibrium or a periodic attractor. To calculate the invasion fitness, a measure of invasion success, we linearize the entire system (9) around the periodic attractor of the resident strain, and compute the stability threshold of the decoupled periodic system of invaders:

$$\begin{aligned}
\frac{dL_{m,1}(t)}{dt} &= \beta(t)S_r(t)I_{m,1}(t) - n\theta_m^{-1}L_{m,1}(t) - bL_{m,1}(t) \\
\frac{dL_{m,j}(t)}{dt} &= n\theta_m^{-1}L_{m,j-1}(t) - n\theta_m^{-1}L_{m,j}(t) - bL_{m,j}(t), \quad j = 2,\dots n \\
\frac{dI_m(t)}{dt} &= n\theta_m^{-1}L_{m,n}(t) - (r+b)I_m(t),
\end{aligned} \tag{10}$$

where $S_r(t)$ is the susceptible component of the periodic attractor. Based on Floquet theory, we develop a numerical algorithm to calculate the invasion fitness. Then we produce PIP by calculating invasion fitnesses for each given parameter pair (θ_r, θ_m). We designate white color for the parameter region with negative invasion fitness, and dark gray color for the region with positive invasion fitness. For the parameter region where residents go extinct, light gray color is designated.

From each PIP having various season lengths, we identify at most two evolutionarily stable and convergence strategies (CSSs), the short CSS and the long CSS. As the season length decreases, the magnitude of long CSS increases, see Figure 5. The biological interpretation of this is that short season length leads to longer latency.

If we overlap the second PIP in Figure 5 with its reflected image over the main diagonal, there exist a region where it is gray in both plots. The region is shown in Figure 6**a** with black color. Two different traits from

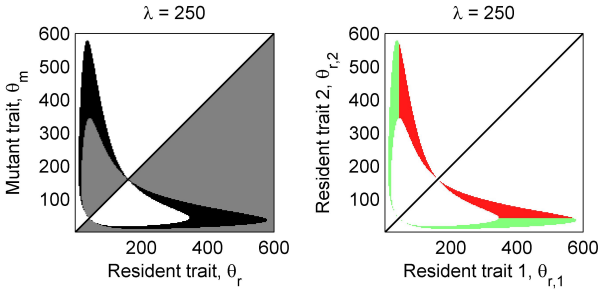

Figure 6: **Two different trait can coexist as a temporal phase of evolutionary process leading to monomorphism. a**, A pair of traits from the black region is mutually invadable and coexist. **b**, Classification of the parameter region of coexistence depending on their long-term evolutionary outcome. Coexisting traits in the green region would converge to long CSS, while the traits in the red region converge to short CSS.

this region can mutually invade each other and consequently coexist. We investigate the long-term evolutionary result of the coexistence, by studying an invasion fitness of mutants when the resident population is settled with two different coexisting traits, $\theta_{r,1}$ and $\theta_{r,2}$.

Figure 6**b** distinguishes the parameter region of coexistence depending on their long-term evolutionary outcome. The coexisting traits in the green region would converge to long CSS, while the traits in the red region converge to short CSS. In conclusion, the observed coexistence of short and long latency strains is predicted to be evolutionarily unstable, though it is epidemiologically stable.

REFERENCES

[1] Hal L. Smith and Horst R. Thieme. *Dynamical systems and population persistence*, volume 118. American Mathematical Soc., 2011.

[2] Wendi Wang and Xiao-Qiang Zhao. Threshold dynamics for compartmental epidemic models in periodic environments. *Journal of Dynamics and Differential Equations*, 20(3):699–717, 2008.